THE JOURNAL OF PHYSICAL CHEMISTRY A

Article

Cite This: J. Phys. Chem. A 2019, 123, 7847−7854

pubs.acs.org/JPCA

Combination Rules and Accurate van der Waals Force Field for Gas Uptakes in Porous Materials

Li Yang,[†,§] Lei Sun,[‡] and Wei-Qiao Deng*[,†,‡]

[†]State Key Laboratory of Molecular Reaction Dynamics, Dalian Institute of Chemical Physics, Chinese Academy of Sciences, Dalian 116023, China

[‡]Institute of Molecular Sciences and Engineering, Shandong University, Qingdao 266237, China

[§]University of the Chinese Academy of Sciences, Beijing 100039, China

Supporting Information

ABSTRACT: Morse function is suggested to be more suitable for studying the gas adsorption in porous frameworks than the Lennard-Jones and exponential-6 forms. However, there have not been some widely used Morse-based van der Waals force fields (vdW FFs) because of complicated parameterization. Combining rules is usually suggested to reduce the parameterization by calculating the unlike-pair parameters from the information of the like pair. A new set of combination rules (DRS) for Morse-based FF has been proposed in our prior work and shown good performance in the simulation of CH_4 adsorption isotherms in covalent organic frameworks. Inspired by our prior work, we developed an accurate van der Waals FF using high-level ab initio calculations with the DRS combination rules. The validation was conducted by comparing the simulated gas uptakes with the experimental values for various known porous materials. The agreement between simulations and experiments is very good, showing the potential application of the FF and the DRS combination rules.

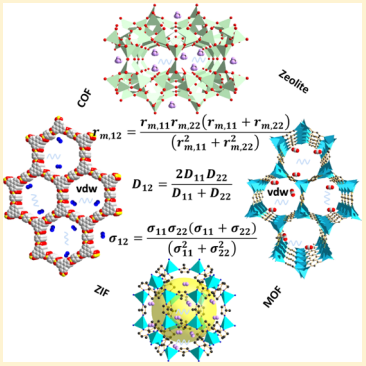

1. INTRODUCTION

Recently, covalent organic frameworks (COFs) together with metal−organic frameworks (MOFs) and other porous materials have attracted significant interest due to their versatility and unique property. The known outstanding qualities of these materials are excellent gas adsorption and separation for the high surface area, exceptional porosity, and topological diversity.[1−5] However, the selection of suitable porous materials for gas adsorption and separation is a significant challenge because of various framework structures. Experimental investigation of adsorption and separation in porous materials is limited because it is time consuming. Thus, molecular simulation has become an important complement to experiments in the screening and selection of suitable porous materials.[6]

Successful conduction of gas adsorption simulation demands force fields (FFs) to describe the intermolecular interactions accurately, especially the van der Waals (vdW) interactions. The vdW interaction in the FFs is a combination of repulsion and attraction, which is different from the usual dispersion. Generic FFs are widely used, but their accuracy is not always satisfactory for gas uptakes. Pérez-Pellitero et al. studied the adsorption of CO_2, CH_4, and N_2 in zeolite imidazolate framework (ZIFs) and found that both universal (UFF)[7] and Dreiding[8] force fields overestimated the isotherms for CH_4 and CO_2 on ZIF-69 and ZIF-8.[9] In addition, our prior work found that Dreiding systematically underestimated uptake of gases, such as H_2, CH_4, CO_2, and N_2, in porous materials, while UFF systematically overestimated compared with the experimental data.[10] Therefore, developing a more reliable FF is important. Since intermolecular interactions can be accurately calculated by ab initio approaches, quantum mechanical (QM) approaches are widely used to develop FFs. In most of the derived FFs, the conventional Lennard-Jones (L-J 12-6) potential is often used to describe the vdW interaction, while Morse potential is usually used to describe the bonded interaction.[11,12] However, studies have proved that the Morse potential model can also be used to describe the vdW interaction and reproduces short- and intermediate-range intermolecular interactions accurately.[10,13−17] Hart declared that conventional functional forms (L-J 12-6 and Exponential-6) possess the wrong shape in the repulsion region.[14] Our recent work also proved this view and found that the L-J 12-6 potential failed in the simulation of gas density at a higher pressure where the repulsive interaction plays a major role.[10,17] Although it is well-known that the Morse potential possesses wrong asymptotic characteristics, these may not be significant in the simulation of gas adsorption in porous materials. Based on this consideration, many works suggest using Morse potential to simulate gas adsorption behaviors in porous materials, as the vdW interaction energy is mainly determined by the short and intermediate range in these cases. In 2010, Goddard III et al. used Morse potential to predict the CH_4 adsorption isotherms for covalent organic frameworks

Received: March 4, 2019
Revised: August 11, 2019
Published: August 20, 2019

DOI: 10.1021/acs.jpca.9b02055
J. Phys. Chem. A 2019, 123, 7847−7854

(COFs).[15] Simulation results show that COF-102 and COF-103 are excellent materials for practical methane storage. Han et al. developed accurate Morse-based vdW FFs for predicting the CO_2 uptakes in MOFs and ZIFs and suggested a strategy for improving the CO_2 uptakes.[16]

Although all of these works are of great importance in gas adsorption simulations, the involved atom types are limited by the complicated parameterization process in developing a Morse-based FF. The general method to solve the problem of complicated parameterization is to introduce combinatorial rules. Three parameters need to be fitted for the Morse potential, which are more than two parameters needed for the L-J 12-6 form, thus making the parameterization more difficult and the use of combination rules more necessary. However, most of the popularly used combination rules are proposed for the L-J 12-6 potential, while only few combination rules are proposed for the Morse potential. Saxena et al. first proposed a simple set of combination rules for the Morse potential and used it to predict the properties of gaseous mixtures.[18] They found that their combination rules were reliable to represent the equilibrium properties of some gaseous mixtures. Later, Saran simplified the forms of Saxena et al. and achieved the same goals.[19] However, the successes of these combination rules are somewhat dependent on the mixture systems considered. Thus, Chang Loyoul Kong developed a more fundamental set of combination rules in 1973 and found that it was superior to the other two sets of rules in predicting the second virial coefficients (B_{12}) of Ne−Kr and Ne−Ar mixtures.[20] However, the forms of rules by Chang Loyoul Kong are too complicated to be used in more realistic applications. In view of this problem, our group developed a new set of combination rules named DRS in prior work and tested it by predicting the second virial coefficients of the mixtures of noble gases.[17] The new set of combination rules has simple forms and shows great performance in all the test systems without any single case of a serious failure.

In this work, we developed a vdW force field with DRS combination rules for gas uptake simulations in zeolites, COFs, MOFs, and ZIFs, and validate the FF parameters by comparing the simulated and experimental uptake of gases in several representative porous materials. In addition, we explored the adsorption behavior of H_2 in IRMOF-1 and IRMOF-3. The results demonstrate that open metal sites are favorable binding sites in the two IRMOFs. Although the FF parameters are not specifically fitted to those particular systems, the agreements between vdW FF simulations and experiments seem to be excellent, showing the potential application of the vdW FF based on the DRS combination rules in exploring gas uptakes in porous materials.

2. METHODS

2.1. Nonbonded Interaction Potentials and Combination Rules. The nonbonded interaction is composed of the vdW interaction and electrostatic interaction. Morse potential is used to approximate the vdW interaction. The form is

$$U_{ij}^{\mathrm{Morse}}(r_{ij}) = D\{\exp[\alpha(1 - r_{ij}/r_{\mathrm{m}})] - 2\exp[\alpha/2(1 - r_{ij}/r_{\mathrm{m}})]\} \quad (1)$$

where D is the well depth, r_{m} is the well depth position, and α determines the curvature of the potential at the minimum as well as the steepness of the repulsive potential. σ is the distance when $U_{ij}^{\mathrm{Morse}}(\sigma_{ij}) = 0$. σ, r_{m}, and α are related to each other according to the relation of eq 2.

$$\sigma = r_{\mathrm{m}}(1 - 2\ln 2/\alpha) \quad (2)$$

The DRS combination rules for the three parameters, D, r_{m}, and σ, are given by eqs 3−5, respectively.[17]

$$D_{12} = \frac{2D_{11}D_{22}}{D_{11} + D_{22}} \quad (3)$$

$$\sigma_{12} = \sigma_{11}\sigma_{22}(\sigma_{11} + \sigma_{22})/(\sigma_{11}^2 + \sigma_{22}^2) \quad (4)$$

$$r_{\mathrm{m},12} = r_{\mathrm{m},11}r_{\mathrm{m},22}(r_{\mathrm{m},11} + r_{\mathrm{m},22})/(r_{\mathrm{m},11}^2 + r_{\mathrm{m},22}^2) \quad (5)$$

For electrostatic interaction, Coulomb potential was used.

$$U_{\mathrm{Coulomb}} = \frac{q_i q_j}{4\pi\varepsilon_0 r_{ij}} \quad (6)$$

where q_i and q_j are the electric charges of atoms i and j obtained from the QM calculations. R_{ij} is the distance between the atoms i and j and ε_0 is the electrical permittivity.

2.2. High-Level Ab Initio Calculations and FF Fitting. We developed the parameters (D, r_{m}, and α) by fitting the QM results. Twenty binary clusters considered in this study are listed in Table S1. Twenty-two like-pair interaction parameters from the 20 binary clusters are listed in Table 1, thus 231 sets of unlike-pair interaction parameters were obtained (see Supporting Information Table S2). The QM-binding energies of CH_4−CH_4, N_2−N_2, H_2−H_2, CO−CO, C_2H_2−C_2H_2, C_2H_4−C_2H_4, O_2−O_2, and NH_3−NH_3 are calculated at the CCSD(T) level,[21,22] while MP2[23−27] was used for other binary systems. Although the CCSD(T) method is more accurate than the MP2 method for vdW interaction, clusters like $Al(OH)_3(H_2O)$−$Al(OH)_3(H_2O)$ are too expensive to be calculated with the CCSD(T) method. Thus, we choose a

Table 1. Like-Pair Morse FF Parameters Developed from the QM Data

atom type	D (kcal/mol)	r_{m} (Å)	α	ref
H___b	0.0235	3.250	10.600	10
H_	0.0478	2.800	11.000	17
C_1	0.0578	5.010	7.000	this work
C_2	0.0934	3.960	10.400	this work
C_3	0.0550	4.900	9.000	17
C_R	0.1139	3.990	11.400	17
N_1	0.0799	3.791	12.546	this work
N_2	0.1366	4.424	10.242	this work
N_3	0.1673	4.684	9.998	this work
N_R	0.2415	3.241	11.587	this work
O_1	0.1227	3.280	18.000	this work
O_2	0.1555	3.170	12.100	10
O_R	0.7177	2.090	19.800	17
O_3_z	0.1234	3.380	11.000	this work
Si3	0.2392	4.000	18.000	17
B_2	0.0978	3.840	14.500	17
Al3	0.0911	5.500	9.800	this work
Na	1.0916	3.300	7.100	this work
Mg3+2	0.6141	3.866	6.179	this work
Zn3+2	1.1418	3.893	10.644	this work
Co6+3	8.8863	2.735	8.885	this work
Ni4+2	7.1833	2.871	10.016	this work

DOI: 10.1021/acs.jpca.9b02055
J. Phys. Chem. A 2019, 123, 7847−7854

more economical MP2 method to calculate the binding energies of larger clusters. A QZVPP basis set was used.[28] All binding energies in the binary systems were corrected using the basis-set superposition error by the full counterpoise procedure.[29,30] The QM calculations were performed using the Gaussian 09 code.[31] In the fitting procedure, we bring the DRS combination rules in the fitting. Thus, only the like-pair parameters are fitted, while the unlike-pair parameters are calculated with the DRS combination rules, which simplified the parameterization greatly. The Gradient Descent method was used to solve the fitting in a multidimensional space. The compiled fitting codes and a simple example of CO can be found in Supporting Information. The energy as a function of distance from the QM calculation and FF fitting are given in the Supporting Information. The root-mean-square deviation (RMSD) of all fits at the minimum is 1.14 kJ/mol.

We selected 15 heterodimers that are important for the description of interactions between porous frameworks and gas molecules to test the accuracy of the unlike-pair parameters (Table S1) directly calculated with combination rules. It consists of 969 binding energies calculated at the MP2/QZVPP level, which includes $Co(OH)_3(H_2O)-(N_2, CO_2, H_2)$, $Mg(OH)_2(H_2O)_3-(CO, H_2, CO_2, N_2)$, $Zn(OH)_2(H_2O)_2-(CO_2, N_2, H_2)$, $B_3O_3H_3-(CO_2, N_2)$, and $C_6H_6-(CO_2, H_2)$. The information about the 969 structures can be found in the Supporting Information. A linear relationship between the QM and fitted FF energy is obtained as given in Figure 1, with a correlation coefficient of 0.95. The correlations between the QM energy and the energy calculated with the FF parameters can reveal the quality of the obtained unlike-pair parameters. It is further suggested that the DRS combination rules could be credible to be used to generate unlike-pair parameters.

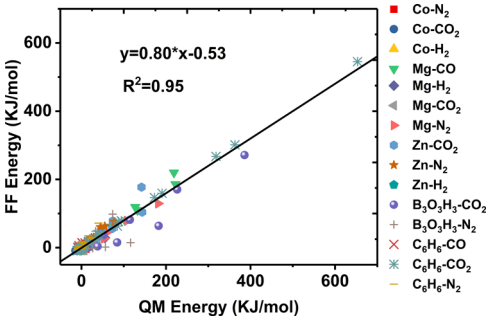

Figure 1. Correlations between the QM energy and FF energy for the vdW interactions between heterodimers.

2.3. Grand canonical Monte Carlo (GCMC) Procedure. Grand canonical Monte Carlo (GCMC) method was used to determine the gas storage capacity and the gas density at different pressures. To ensure an accurate measurement of molecular loading, we ran 10 000 000 equilibration steps in the equilibrium stage and 10 000 000 Monte Carlo steps in the production stage. These simulations used zeolites (FER and LTA[32]), ZIFs (ZIF-8[33] and ZIF-9[34]), MOFs (IRMOF-1,[35] IRMOF-3,[35] IRMOF-6,[35] M-MOF-74 (M: Mg, Co, Ni, and Zn)[36−38]), and COF-5.[39] The influence of the framework charge on the CO_2 uptake cannot be ignored. For a reliable simulation of the CO_2 uptakes, atomic charges of CO_2 were determined by the Mulliken population using the HF density, while those of the frameworks of COF-5 and LTA were obtained by the Mulliken population from the DFT calculations. The DFT calculations were performed by the DMol3 package[40−42] using a PBE (Perdew, Burke, and Enzerhof) functional[43] and a double-numeric quality basis set with polarization functions (DND). The charges of M-MOF-74 (M: Mg, Co, Ni, Zn) frameworks were referred from Pham et al.[44] The density of different gases at different pressures was analyzed in a 10 × 10 × 10 Å^3 box using the sorption module of Cerius2 software.[45]

3. RESULTS AND DISCUSSION

3.1. Gas Density Simulation. To validate the parameters developed by the new combination rules, we first compared the predicted gases density with the experimental data from the National Institute of Standards and Technology. The predicted densities of C_2H_4 and CO_2 are shown in Figure 2b,d together with the energy curves as a function of distance (Figure 2a,c). Here, we used the Mulliken atomic charges for the electrostatic potential that were derived from the QM calculations. The atomic charges for C_2 and H_ in C_2H_4 are −0.2028 and 0.1014, respectively, while those for C_1 and O_2 in CO_2 are 0.572 and −0.286, respectively. At the minimum, the fitting percentage error is 1.1% (QM: −5.48 kJ/mol, FF: −5.54 kJ/mol) for C_2H_4 and 19.2% (QM: −4.24 kJ/mol, FF: −3.43 kJ/mol) for CO_2. The FF parameters reproduce reasonably well the QM binding energies for C_2H_4. The percentage error for the CO_2 energy curve at the minimum is somewhat large as shown in the inset in Figure 2c, but it is acceptable to take into account that three configurations are used in the fitting. Root-mean-square deviation (RMSD) of the attractive points for $C_2H_4-C_2H_4$, CO_2-CO_2, and other 12 like-pair systems are listed in Table S3. Most of the RMSD are below 1 kJ/mol (0.19−0.88 kJ/mol). The max RMSD was found in the fitting of $C_3NH_5-C_3NH_5$ (2.03 kJ/mol), but this deviation is not significant considering that the most stable interaction is 12.38 kJ/mol. Our new FF parameters (Tables 1 and S2) reproduce well these repulsive and attractive binding energies as shown in Table S3, Figures 2a,c, and S1−S12. In Figure 2b, the C_2H_4 density was simulated from 1 to 100 bar. The predicted C_2H_4 density using the new vdW parameters at 100 bar is 332.94 kg/m^3, which is well in agreement with the value of 330.63 referenced from the NIST. However, the predicted C_2H_4 density both by UFF and Dreiding significantly deviates from the experimental values (512 kg/m^3 for UFF and 85 kg/m^3 for Dreiding). In Figure 2d, we simulated the CO_2 density at 298 K. As CO_2 undergoes a phase transformation above 70 bar, the simulation was conducted from 1 to 60 bar. The relative errors of the simulated density with UFF and Dreiding FFs are 50 and 36%, while that with vdW FF is 5%, when the pressure reaches the phase transformation point. Compared with UFF and Dreiding FFs, the vdW FFs are more reliable for predicting the gas density.

3.2. Gas Uptakes in Porous Materials. To validate the reliability of the FF parameters, we further conducted GCMC simulations for various kinds of porous materials including zeolites, MOFs, COFs, and ZIFs. We compared the simulated gas uptakes in these porous materials with the experimental values.

Figure 3a,b shows excess CH_4 adsorption isotherms in FER and IRMOF-6. The predicted excess uptake in FER of 13.49 mg/g at 0.9 bar and 309 K is very close to the experimental result of 13.76 mg/g at 0.9185 bar and 309 K (Figure 3a).[46] The UFF and Dreiding apparently overestimated the

DOI: 10.1021/acs.jpca.9b02055
J. Phys. Chem. A 2019, 123, 7847−7854

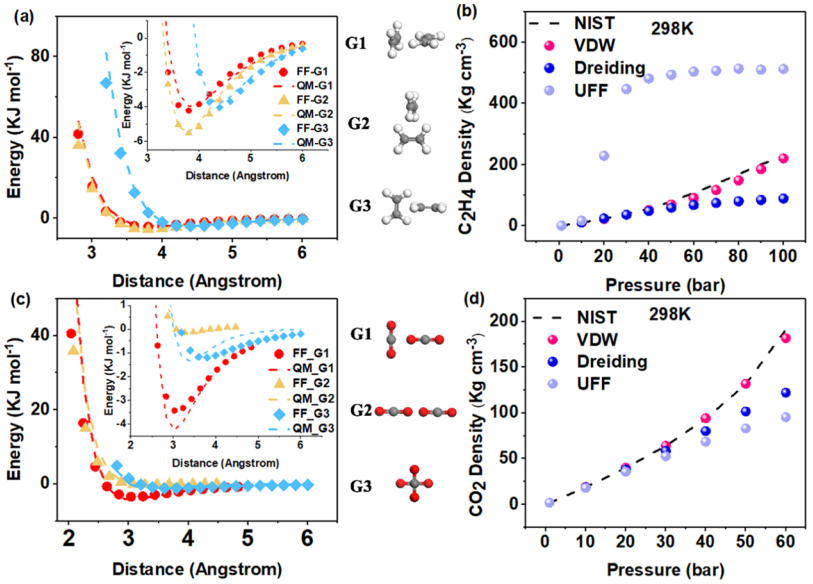

Figure 2. Comparison of the fitted FF (FF) energies with QM results: (a) C_2H_4−C_2H_4 and (c) CO_2−CO_2. Density calculated by a combination of GCMC simulations and the developed FF parameters: (b) C_2H_4−C_2H_4 and (d) CO_2−CO_2. Here, C atoms are brown, O red, and H white. The insets show the accuracy in fitting to the equilibrium distance.

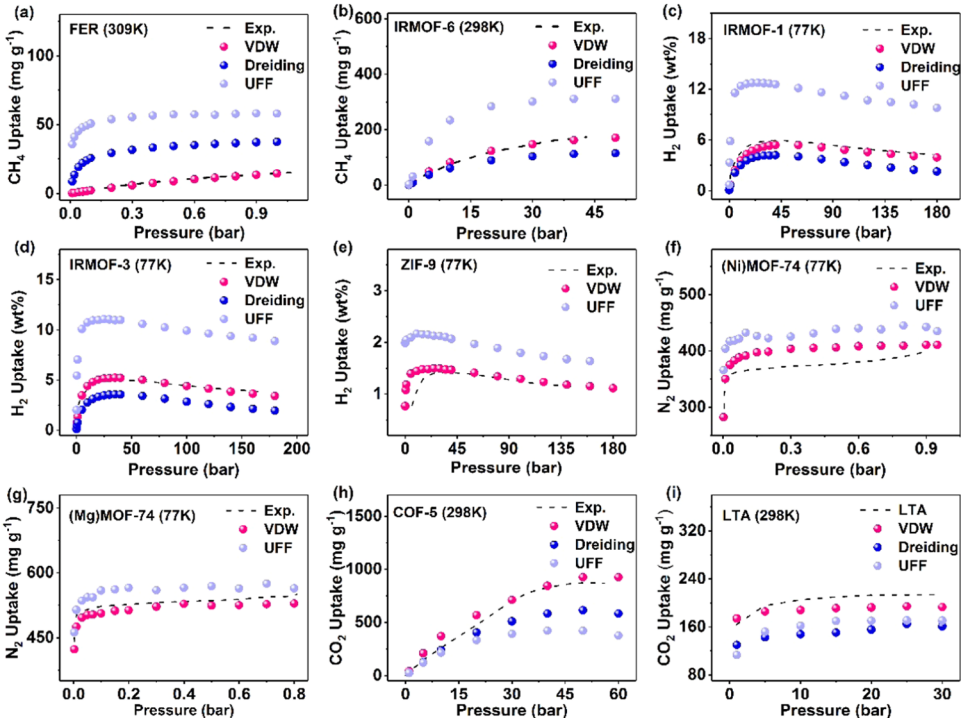

Figure 3. Predicted (symbols) and experimental (dashed lines) excess uptake isotherms.

adsorption value; besides, the adsorption trend was not right. In Figure 3b, the methane sorption isotherm of IRMOF-6 was simulated in the pressure range 0.1−50.0 bar and temperature 298 K. The predicted excess methane uptake in IRMOF-6 is 226.8 cm^3 (standard temperature and pressure STP)/g (151.2 mg/g) at 40 bar, in excellent agreement with the experimental value of 240 cm^3(STP)/g (171 mg/g) at 298 K and 36.5 bar.[35] The excess uptakes calculated using UFF are 435.2 and 156.3 cm^3(STP)/g for IRMOF-6 at 40 bar and 298 K, which lead to serious discrepancies. Dreiding underestimated the CH_4 uptake in IRMOF-6. The CH_4 uptakes in COFs (COF-5, COF-10, COF-12, and COF-13) was conducted in our prior work, which also showed great agreement with the experimental values.[17] The simulated results suggest that our FF parameters developed using the new combination rules provide a good estimation of the methane uptakes in different porous materials.

We have computed the adsorption isotherms for H_2 in MOFs and ZIFs and compared the simulation data with the experimental results shown in Figure 3. In the case of IRMOFs, we see from Figure 3c,d that the simulations using the vdW force field agree very well with the experimental data. The

DOI: 10.1021/acs.jpca.9b02055
J. Phys. Chem. A 2019, 123, 7847−7854

Table 2. Maximum Excess Uptakes and Pressure of Materials

	pressure (bar)				maximum excess uptakes (wt %)			
material name	exp.	vdW	Dreiding	UFF	exp.	vdW	Dreiding	UFF
IRMOF-1	40.1	40.0	40.0	40.0	5.93	5.40	4.20	12.76
IRMOF-3	40.7	40.0	40.0	40.0	5.02	5.22	3.56	11.07
ZIF-8	32.2	30.0	30.0	30.0	3.46	2.99	2.47	5.77
ZIF-9	38.6	40.0		40.0	1.37	1.47		2.06

Table 3. Simulated and Experimental Heats of Adsorption (in kJ/mol)

			calcd		
porous materials	gas	exp.	vdW	UFF	others
Mg-MOF-74	CO_2	39,[53] 47,[54] 42,[55] 44[56]	39.0	32.6	41,[56] 38[57]
	N_2	18,[54] 21[57]	15.7	13.5	25[57]
Co-MOF-74	CO_2	34,[56] 37[54]	35.7	29.2	34[56]
Ni-MOF-74	CO_2	39,[56] 41[54]	35.4	32.3	37[56]
Zn-MOF-74	CO_2	27[56]	25.4	25.6	30,[56] 32[58]

simulated maximum excess of IRMOF-1 is 5.40 wt % at 40.0 bar, which is very close to the experimental value of 5.93 wt % at 40.1 bar.[47] The simulated maximum excess of IRMOF-3 of 5.22 wt % at 40.0 bar is also in excellent agreement with the experimental value of 5.02 wt % at 40.7 bar.[47] The predicted results using UFF are twice as high as the experimental values, while the simulated values of Dreiding are a bit underestimated. In Figure 3e, we compare the predicted excess H_2 uptake in ZIF-9(Co) with the experimental. The vdW FFs somewhat overestimate the H_2 uptakes at lower pressure, but fit very well with the experiment values when the pressure increased. The experimental hydrogen uptake for ZIF-9 at 38.6 bar is 1.37 wt %.[47] The simulated hydrogen uptake with vdW FF for ZIF-9 at 40.0 bar is 1.47 wt %. The two values are very close. Because there is no Co, Mg, and Ni element in the Dreiding FF, Figure 3e–g only compares the vdW FF with UFF. The UFF result at 40.0 bar is 2.06 wt % for ZIF-9, which is an obvious overestimation of the hydrogen adsorption capability of ZIF-9. We compared the predicted excess H_2 uptake in ZIF-8(Zn) with the experimental values in Figure S13.[47] The uptake of H_2 is underestimated in ZIF-8 whether using vdW or Dreiding FF. However, the predicted pressure (30.0 bar) corresponding to the maximum excess uptake is very close to the experimental value (32.2 bar). Both FFs reproduce the corrected adsorption trends of H_2 in ZIF-8. In general, the adsorption capacity of H_2 simulated by UFF is obviously higher than the experimental value, which is almost twice the experimental value. In addition, the predicted maximum excess uptake pressure is systematically lower than the experimental result. Explicitly, the simulated and experimental maximum excess uptake and the corresponding pressure for each material are listed in Table 2.

Figure 3f,g compares the predicted excess N_2 adsorption isotherms for Ni-MOF-74 and Mg-MOF-74 with the experimental results.[2] In Figure 3g, the simulated N_2 uptakes in Mg-MOF-74 with vdW FF are clearly closer to the experiment values than to the UFF FF. Although the predicted N_2 adsorption isotherms in Ni-MOF-74 are somewhat higher than the experiment values for both FFs, the vdW FF reproduces the experimental value better than UFF does. In Figure 3i, we compare the theoretical simulation of the CO_2 adsorption capacity in the silicon–aluminum zeolite LTA (contain Na^+) with the experimental data.[48] The predicted results show that the uptakes simulated using UFF, Dreiding, and vdW FF are very similar. However our vdW FF reproduces the experimental changing trend better than the others. Similarly, Figure 3h shows that the vdW FF also reproduced the excess CO_2 adsorption isotherm for COF-5 better than UFF and Dreiding FF did compared with the experimental results.[49]

We found that the newly developed vdW FF parameters with the DRS combination rules yielded the best overall agreement with the experimental gas densities and adsorption isothermals, particularly at higher pressures. The deviation between the experimental and computed gas densities with generic FFs UFF and Dreiding starts small and increases with increasing pressures, as seen in Figure 2b,d. One possible explanation could be that the accuracy of the parameters of the generic FFs is not always satisfactory for porous materials. In addition, the L-J 12-6 form used in the generic FFs is too stiff to describe the repulsion region of vdW interactions. Although it is generally considered that the conformations near the potential well are more important, the repulsive interaction will play an important role in the simulations of gas densities and uptakes when the pressure increases. Another, perhaps more important, reason is that the Lorentz–Berthelot (LB) combination rules used in the generic FFs may not be reliably suited for gas adsorption simulation. Although the LB combination rules used in the UFF and Dreiding FFs are by far the oldest and most common approach, there are works that reported that it led to inaccurate mixture properties for some systems.[50−52] Additional evidence also can be found in our previous work.[16] The deviations between the predicted and experimental gas densities using the UFF and Dreiding FFs are not significant when used in the simulation of the gas densities of molecules like N_2, O_2, and H_2 (except for the H_2 density simulated using UFF), which only contain like-pair parameters but significant when used in the systems (CH_4, C_2H_4, and CO_2), which contain unlike-pair parameters calculated with the LB rules.

3.3. Isosteric Heat of Adsorption. The heat of adsorption (Q_{st}) is one of the most important surface characteristics used to evaluate the adsorption performance of porous materials and can be calculated from the ensemble average of the energy/particle fluctuations in GCMC simulations. As the third test of our force field, we computed the low-coverage CO_2 Q_{st} (a loading smaller than 0.01 of CO_2 per M^{2+}) and compared it with the experimental and simulated

DOI: 10.1021/acs.jpca.9b02055
J. Phys. Chem. A 2019, 123, 7847−7854

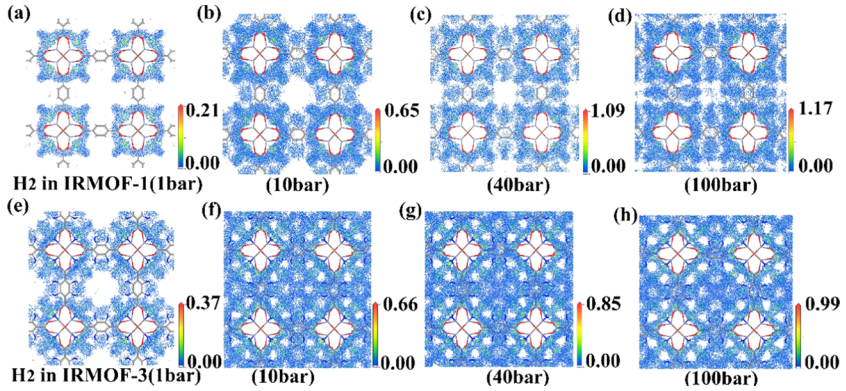

Figure 4. Simulated average density (g/cm^3) colored by field for H_2 in (a)−(d) IRMOF-1 and (e)−(h) IRMOF-3.

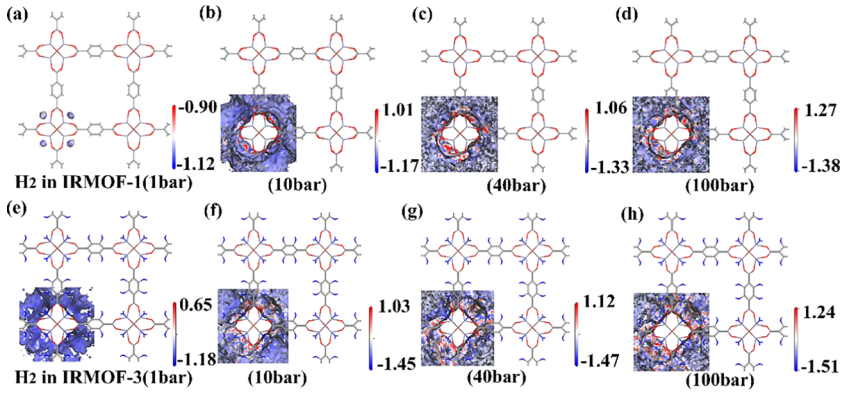

Figure 5. Isodensity surface colored by potential energy for H_2 in (a)−(d) IRMOF-1 and (e)−(h) IRMOF-3.

values of other authors (Table 3).[53−58] Q_{st} determines the interactions between gas molecules and framework. Four isoreticular M-MOF-74 analogues were used here for which there is a huge amount of existing computational data. In Mg-MOF-74, the measured Q_{st} of CO_2 shows that it has a wide range from 39 to 47 kJ/mol.[53−56] The calculated values using vdW force field is 39.0 kJ/mol, which is in agreement with the simulated data of both Queen et al.[56] (41 kJ/mol) and Valenzano et al.[57] (38 kJ/mol) and within the experimental range. In Co-MOF-74, the Q_{st} of CO_2 calculated using vdW FF is also within a tolerable range compared to the measured and simulated values.[54,56] These results indicates that vdW FF gives the correct description of the interaction between CO_2 and the open metal atoms in Mg-MOF-74 and Co-MOF-74. For the Q_{st} of N_2 in Mg-MOF-74 and CO_2 in Ni-MOF-74 and Zn-MOF-74, the obtained vdW values (15.7, 35.4, and 25.1 kJ/mol, respectively) are slightly smaller than the experimental and simulated values.[54−58] As shown in Table 3, the vdW FF calculations significantly improve the accuracy of these Q_{st} calculations over the UFF FF predictions compared with the experimental and simulated Q_{st} of other authors.

3.4. Adsorption Behavior. To explore the adsorption behavior of H_2 in IRMOF-1 and IRMOF-3, the average density obtained from the GCMC simulations was used, as shown in Figure 4a−h. The dot output field represents a density distribution of H_2 molecules in the lattice framework. As shown in Figure 4, the average densities are small at low pressure and increase with rising pressure. At low pressure (Figure 4a,e), hydrogen molecules tend to accumulate in the open metal sites. With the increase of pressure, a small amount of hydrogen molecules accumulate around the benzene and amino groups. The simulation results show that hydrogen molecules have a strong interaction with open metal (Zn) but a relatively weak interaction with benzene and amine. We combine the energy and density distribution information by creating a surface of constant density (isovalue = 0.01) and colored it by potential energy. In Figure 5a−h, blue area has lower energy and red has higher energy. The red region demonstrates that the open metal sites are favorable binding sites in the two IRMOFs, which is consistent with the results from the density field analysis in Figure 4. A comparison of the hydrogen adsorption behaviors in IRMOF-1 and IRMOF-3 shows that the amino group is in the favor of H_2 adsorption.

4. CONCLUSIONS

In summary, we proposed the DRS combination rules for Morse potential in our prior work and tested the reliability by predicting the second virial coefficients of gaseous mixtures. Test results showed that the DRS rules work very well for all the considered mixed binaries without any single serious failure case. We further used the DRS combination rules in deriving the vdW FF parameters and simulate the adsorption isotherms of CH_4 in COFs. The overall agreement was good, which supports further applications of this new set of combination rules in more realistic simulation systems. Therefore, we extended our previous efforts of deriving vdW FFs parameters for adsorption of gases from high-level ab initio calculations in porous materials. Using the derived FF, we simulated the densities of gases and their uptakes in COFs, MOFs, ZIFs, and zeolite using the GCMC method. The simulation results are in good agreement with the experimental results, which supports

DOI: 10.1021/acs.jpca.9b02055
J. Phys. Chem. A 2019, 123, 7847−7854

the further use of vdW FF and the DRS combination rules in gas adsorption simulations.

■ ASSOCIATED CONTENT

Supporting Information

The Supporting Information is available free of charge on the ACS Publications website at DOI: 10.1021/acs.jpca.9b02055.

Parameter file (VDW.txt); compiled fitting code and a simple fitting example of CO; Structures used in this work (ZIP)

Force field type and parameters of vdW FF (Section S1); force field type in each molecular cluster (Table S1); unlike-pair Morse force field parameters developed from QM data in this work (Table S2); RMSD of the attractive points (Table S3); comparison of fitted FF (point) energies with QM (curve) for Al-$(OH)_3(H_2O)$–$Al(OH)_3(H_2O)$, Co$(OH)_3$(H2O)–Co-$(OH)_3(H_2O)$, $Si(OH)_4$–$Si(OH)_4$, Ni-$(OH)_2(H_2O)_2$–$Ni(OH)_2(H_2O)_2$, Na(OH)-$(H_2O)_3$–$Na(OH)(H_2O)_3$, $Zn(OH)_2(H_2O)_2$–Zn-$(OH)_2(H_2O)_2$, $C_3N_3H_3$–$C_3N_3H_3$, C_3NH_5–C_3NH_5, N_2–N_2, NH_3–NH_3, $Mg(OH)_2(H_2O)_3$–Mg-$(OH)_2(H_2O)_3$ and CO–CO dimers (Figure S1–S12); H2 uptakes in ZIF-8 (Figure S13); Comparison of simulated and experimental adsorption isotherms and Q_{st} of CO_2 in Mg-MOF-74 (Figure S14); reproduce the results with other open source software (Section S3) (PDF)

■ AUTHOR INFORMATION

Corresponding Author

*E-mail: dengwq@dicp.ac.cn

ORCID

Wei-Qiao Deng: 0000-0002-3671-5951

Notes

The authors declare no competing financial interest.

■ ACKNOWLEDGMENTS

This work was supported by the Fundamental Research Funds of Shandong University, the National Key Research and Development Program of China (No. 2017YFA0204800), National Science and Technology Major Project of the Ministry of Science and Technology of China (No. 2017ZX05036001), Chinese Academy of Sciences (No. XDB10020201), and National Natural Science Foundation of China (Nos. 21525315 and 91333116).

■ REFERENCES

(1) Furukawa, H.; Yaghi, O. M. Storage of Hydrogen, Methane, and Carbon Dioxide in Highly Porous Covalent Organic Frameworks for Clean Energy Applications. *J. Am. Chem. Soc.* **2009**, *131*, 8875–8883.

(2) Dietzel, P. D. C.; Georgiev, P. A.; Eckert, J.; Blom, R.; Strassle, T.; Unruh, T. Interaction of hydrogen with accessible metal sites in the metal-organic frameworks M_2(dhtp) (CPO-27-M; M = Ni, Co, Mg). *Chem. Commun.* **2010**, *46*, 4962–4964.

(3) Bao, Z.; Yu, L.; Ren, Q.; Lu, X.; Deng, S. Adsorption of CO_2 and CH_4 on a magnesium-based metal organic framework. *J. Colloid Interface Sci.* **2011**, *353*, 549–556.

(4) Du, T.; Long, Y.; Tang, Q.; Li, S. L.; Liu, L. Y. Adsorption Property of Mg-MOF-74 for CO_2/H_2O. *Chem. J. Chin. U* **2017**, *38*, 225–230.

(5) Vicent-Luna, J. M.; Luna-Triguero, A.; Calero, S. Storage and Separation of Carbon Dioxide and Methane in Hydrated Covalent Organic Frameworks. *J. Phys. Chem. C* **2016**, *120*, 23756–23762.

(6) Fang, H.; Demir, H.; Kamakoti, P.; Sholl, D. S. Recent developments in first-principles FFs for molecules in nanoporous materials. *J. Mater. Chem. A* **2014**, *2*, 274–291.

(7) Rappé, A. K.; Casewit, C. J.; Colwell, K. S.; Goddard, W. A., III; Skiff, W. M. UFF, a Full Periodic Table Force Field for Molecular Mechanics and Molecular Dynamics Simulations. *J. Am. Chem. Soc.* **1992**, *114*, 10024–10035.

(8) Mayo, S. L.; Olafson, B. D.; Goddard, W. A., III DREIDING: A Generic Force Field for Molecular Simulations. *J. Phys. Chem. A* **1990**, *94*, 8897–8909.

(9) Pérez-Pellitero, J.; Amrouche, H.; Siperstein, F. R.; Pirngruber, G.; Nieto-Draghi, C.; Chaplais, G.; Simon-Masseron, A.; Bazer-Bachi, D.; Peralta, D.; Bats, N. Adsorption of CO_2, CH_4, and N_2 on zeolitic imidazolate frameworks: experiments and simulations. *Chem. - Eur. J.* **2010**, *16*, 1560–1571.

(10) Sun, L.; Yang, L.; Zhang, Y. D.; Shi, Q.; Lu, R. F.; Deng, W. Q. Accurate van der Waals force field for gas adsorption in porous materials. *J. Comput. Chem.* **2017**, *38*, 1991–1999.

(11) Haldoupis, E.; Borycz, J.; Shi, H.; Vogiatzis, K. D.; Bai, P.; Queen, W. L.; Gagliardi, L.; Siepman, J. I. Ab Initio Derived Force Fields for Predicting CO_2 Adsorption and Accessibility of Metal Sites in the Metal–Organic Frameworks MMOF-74 (M = Mn, Co, Ni, Cu). *J. Phys. Chem. C* **2015**, *119*, 16058–16071.

(12) Yazaydın, A. O.; Snurr, R. Q.; Park, T. H.; Koh, K.; Liu, J.; LeVan, M. D.; Benin, A. I.; Jakubczak, P.; Lanuza, M.; Galloway, D. B.; Low, J. L.; Willis, R. R. Screening of Metal-Organic Frameworks for Carbon Dioxide Capture from Flue Gas Using a Combined Experimental and Modeling Approach. *J. Am. Chem. Soc.* **2009**, *131*, 18198–18199.

(13) Abraham, R. J. The Morse Curve As a Non-bonded Potential Function. *Chem. Phys. Lett.* **1978**, *58*, 622–644.

(14) Hart, J. R.; Rappé, A. K. van der Waals functional forms for molecular simulations. *J. Chem. Phys.* **1992**, *97*, 1109–1115.

(15) Mendoza-Cortés, J. L.; Han, S. S.; Furukawa, H.; Yaghi, O. M.; Goddard, W. A., III Adsorption Mechanism and Uptake of Methane in Covalent Organic Frameworks: Theory and Experiment. *J. Phys. Chem. A* **2010**, *114*, 10824–10833.

(16) Han, S. S.; Kim, D.; Jung, D. H.; Cho, S.; Choi, S. H.; Jung, Y. Accurate Ab Initio-Based Force Field for Predictive CO_2 Uptake Simulations in MOFs and ZIFs: Development and Applications for MTV-MOFs. *J. Phys. Chem. C* **2012**, *116*, 20254–20261.

(17) Yang, L.; Sun, L.; Deng, W. Q. Combination Rules for Morse-Based van der Waals Force Fields. *J. Phys. Chem. A* **2018**, *122*, 1672–1677.

(18) Saxena, S. C.; Gambhir, R. S. Second virial coefficient of gases and gaseous mixtures on the Morse potential. *Mol. Phys.* **1963**, *6*, 577–583.

(19) Saran, A. Potential Parameters for Like and Unlike Interactions on Morse Potential Model. *Indian J. Phys.* **1963**, *37*, 491–499.

(20) Kong, C. L. Combining rules for intermolecular potential parameters. II. Rules for the Lennard-Jones (12-6) potential and the Morse potential. *J. Chem. Phys.* **1973**, *59*, 2464–2467.

(21) Purvis, G. D., III; Bartlett, R. J. J. A full coupled-cluster singles and doubles model: The inclusion of disconnected triples. *Chem. Phys.* **1982**, *76*, 1910–1918.

(22) Pople, J. A.; Head-Gordon, M.; Raghavachari, K. Quadratic configuration interaction – a general technique for determining electron correlation energies. *J. Chem. Phys.* **1987**, *87*, 5968–5975.

(23) Frisch, M. J.; Head-Gordon, M.; Pople, J. A. Direct MP2 gradient method. *Chem. Phys. Lett.* **1990**, *166*, 275–280.

(24) Frisch, M. J.; Head-Gordon, M.; Pople, J. A. Semi-direct algorithms for the MP2 energy and gradient. *Chem. Phys. Lett.* **1990**, *166*, 281–289.

(25) Head-Gordon, M.; Pople, J. A.; Frisch, M. J. MP2 energy evaluation by direct methods. *Chem. Phys. Lett.* **1988**, *153*, 503–506.

DOI: 10.1021/acs.jpca.9b02055
J. Phys. Chem. A 2019, 123, 7847–7854

(26) Sæbø, S.; Almlöf, J. Avoiding the integral storage bottleneck in LCAO calculations of electron correlation. *Chem. Phys. Lett.* **1989**, *154*, 83−89.
(27) Head-Gordon, M.; Head-Gordon, T. Analytic MP2 Frequencies Without Fifth Order Storage: Theory and Application to Bifurcated Hydrogen Bonds in the Water Hexamer. *Chem. Phys. Lett.* **1994**, *220*, 122−128.
(28) Weigend, F.; Ahlrichs, R. Balanced basis sets of split valence, triple zeta valence and quadruple zeta valence quality for H to Rn: Design and assessment of accuracy. *Phys. Chem. Chem. Phys.* **2005**, *7*, 3297−3305.
(29) Simon, S.; Duran, M.; Dannenberg, J. J. How does basis set superposition error change the potential surfaces for hydrogen-bonded dimers? *J. Chem. Phys.* **1996**, *105*, 11024−11031.
(30) Boys, S. F.; Bernardi, F. The Calculation of Small Molecular Interactions by the Differences of Separate Total Energies. Some Procedures with Reduced Errors. *Mol. Phys.* **1970**, *19*, 553−566.
(31) Frisch, M. J.; Trucks, G. W.; Schlegel, H. B.; Scuseria, G. E.; Robb, M. A.; Cheeseman, J. R.; Montgomery, J. A.; Vreven, T.; Kudin, K. N.; Burant, J. C.;et al. *Gaussian 09*, revision C.01; Gaussian, Inc.: Wallingford, CT, 2009.
(32) Pluth, J. J.; Smith, J. V. Accurate Redetermination of Crystal Structure of Dehydrated Zeolite A. Absence of Near Zero Coordination of Sodium. Refinement of Si,Al-Ordered Superstructure. *J. Am. Chem. Soc.* **1980**, *102*, 4704−4708.
(33) Novaković, S. B.; Bogdanovic, G. A.; Heering, C.; Makhloufi, G.; Francuski, D.; Janiak, C. Charge-density distribution and electrostatic flexibility of ZIF-8 based on high-resolution X-ray diffraction data and periodic calculations. *Inorg. Chem.* **2015**, *54*, 2660−2670.
(34) Zhao, P.; Bennett, T. D.; Casati, N. P.; Lampronti, G. I.; Moggach, S. A.; Redfern, S. A. Pressure-induced oversaturation and phase transition in zeolitic imidazolate frameworks with remarkable mechanical stability. *Dalton Trans* **2015**, *44*, 4498−4503.
(35) Eddaoudi, M.; Kim, J.; Rosi, N.; Vodak, D.; Wachter, J.; O'keeffe, M.; Yaghi, O. M. Systematic Design of Pore Size and Functionality in Isoreticular MOFs and Their Application in Methane Storage. *Science* **2002**, *295*, 469−472.
(36) Dietzel, P. D.; Blom, R.; Fjellvag, H. Base-Induced Formation of Two Magnesium Metal-Organic Framework Compounds with a Bifunctional Tetratopic Ligand. *Eur. J. Inorg. Chem.* **2008**, 3624−3632.
(37) Dietzel, P. D.; Panella, B.; Hirscher, M.; Blom, R.; Fjellvag, H. Hydrogen adsorption in a nickel based coordination polymer with open metal sites in the cylindrical cavities of the desolvated framework. *Chem. Commun.* **2006**, 959−961.
(38) Wong-Ng, W.; Kaduk, J. A.; Wu, H.; Suchomel, M. Synchrotron X-ray studies of metal-organic framework M_2(2,5-dihydroxyterephthalate), M = (Mn, Co, Ni, Zn) (MOF74). *Powder Diffr.* **2012**, *27*, 256−262.
(39) Cote, A. P.; Benin, A. I.; Ockwig, N. W.; O'Keeffe, M.; Matzger, A. J.; Yaghi, O. M. Porous, Crystalline, Covalent Organic Frameworks. *Science* **2005**, *310*, 1166−1170.
(40) Delley, B. An All-Electron Numerical Method for Solving the Local Density Functional for Polyatomic Molecules. *J. Chem. Phys.* **1990**, *92*, 508−517.
(41) Delley, B. A Scattering Theoretic Approach to Scalar Relativistic Corrections on Bonding. *Int. J. Quant. Chem.* **1998**, *69*, 423−433.
(42) Delley, B. From Molecules to Solids With the DMol^3 Approach. *J. Chem. Phys.* **2000**, *113*, 7756−7764.
(43) Perdew, J. P.; Burke, K.; Ernzerhof, M. Generalized Gradient Approximation Made Simple. *Phys. Rev. Lett.* **1996**, *77*, 3865−3868.
(44) Pham, T.; Forrest, K. A.; Banerjee, R.; Orcajo, G.; Eckert, J. Space, B.Understanding the H_2 Sorption Trends in the M-MOF-74 Series (M = Mg, Ni, Co, Zn). *J. Phys. Chem. C* **2015**, *119*, 1078−1090.
(45) *The Cerius2 Software*, version 5.5; Accelrys, Inc.: San Diego, CA, 2009.
(46) Savitz, S.; Siperstein, F.; Gorte, R. J.; Myers, A. L. Calorimetric Study of Adsorption of Alkanes in High-Silica Zeolites. *J. Phys. Chem. B* **1998**, *102*, 6865−6872.
(47) Noguera-Díaz, A.; Bimbo, N.; Holyfield, L. T.; Ahmet, I. Y.; Ting, V. P.; Mays, T. J. Structure-property relationships in metal-organic frameworks for hydrogen storage hydrogen storage. *Colloids Surf., A* **2016**, *496*, 77−85.
(48) Chen, C.; Ahn, W. S. CO_2 adsorption on LTA zeolites: Effect of mesoporosity. *Appl. Surf. Sci.* **2014**, *311*, 107−109.
(49) Furukawa, H.; Yaghi, O. M. Storage of Hydrogen, Methane, and Carbon Dioxide in Highly Porous Covalent Organic Frameworks for Clean Energy Applications. *J. Am. Chem. Soc.* **2009**, *131*, 8875−8883.
(50) Delhommelle, J.; MilliÉ, P. Inadequacy of the Lorentz-Berthelot combining rules for accurate predictions of equilibrium properties by molecular simulation. *Mol. Phys.* **2001**, *99*, 619−625.
(51) Ungerer, P.; Wender, A.; Demoulin, G.; Bourasseau, É.; Mougin, P. Application of Gibbs ensemble and NPT Monte Carlo simulation to the development of improved processes for H_2S-rich gases. *Mol. Simul.* **2004**, *30*, 631−648.
(52) Schnabel, T.; Vrabec, J.; Hasse, H. Unlike Lennard-Jones parameters for vapor-liquid equilibria. *J. Mol. Liq.* **2007**, *135*, 170−178.
(53) Dietzel, P. D.; Besikiotis, V.; Blom, R. Application of metal−organic frameworks with coordinatively unsaturated metal sites in storage and separation of methane and carbon dioxide. *J. Mater. Chem.* **2009**, *19*, 7362−7370.
(54) Caskey, S. R.; Wong-Foy, A. G.; Matzger, A. J. Dramatic tuning of carbon dioxide uptake via metal substitution in a coordination polymer with cylindrical pores. *J. Am. Chem. Soc.* **2008**, *130*, 10870−10871.
(55) Mason, J. A.; Sumida, K.; Herm, Z. R.; Krishna, R.; Long, J. R. Evaluating metal−organic frameworks for post-combustion carbon dioxide capture via temperature swing adsorption. *Energy Environ. Sci.* **2011**, *4*, 3030−3040.
(56) Queen, W. L.; Hudson, M. R.; Bloch, E. D.; Mason, J. A.; Gonzalez, M. I.; Lee, J. S.; Howe, D. J.; Lee, K.; Darwish, T. A.; James, M.; Peterson, V. K.; Teat, S. J.; Smit, B.; Neaton, J. B.; Long, J. R.; Brown, C. M.; et al. Comprehensive study of carbon dioxide adsorption in the metal−organic frameworks M_2 (dobdc)(M = Mg, Mn, Fe, Co, Ni, Cu, Zn). *Chem. Sci.* **2014**, *5*, 4569−4581.
(57) Valenzano, L.; Civalleri, B.; Chavan, S. A.; Palomino, G. T.; Areán, C. O.; Bordiga, S. Computational and Experimental Studies on the Adsorption of CO, N_2, and CO_2 on Mg-MOF-74. *J. Phys. Chem. C* **2010**, *114*, 11185−11191.
(58) Dzubak, A. L.; Lin, L. C.; Kim, J.; Swisher, J. A.; Poloni, R.; Maximoff, S. N.; Smit, B.; Gagliardi, L. Ab initio carbon capture in open-site metal−organic frameworks. *Nat. Chem.* **2012**, *4*, No. 810.

DOI: 10.1021/acs.jpca.9b02055
J. Phys. Chem. A 2019, 123, 7847−7854